Very long wavelength type-II InAs/GaSb superlattice infrared detectors

L. Höglund[1], J. B. Rodriguez[2], S. Naureen[1], R. Ivanov[1], C. Asplund[1], R. Marcks von Würtemberg[1], R. Rossignol[2], P. Christol[2], A. Rouvié[3], J. Brocal[3], O. Saint-Pé[3], E. Costard[1]

[1]IRnova AB, Isafjordsgatan 22 C5, SE-16440 Kista, Sweden
[2] IES, Université de Montpellier, CNRS, F- 34000, Montpellier, France
[3]Airbus Defence and Space, 31 Rue des Cosmonautes, ZI du Palays, 31402 Toulouse, France

ABSTRACT

In this paper, results from the development of LWIR and VLWIR InAs/GaSb type-II infrared photodetector arrays are presented. Dark currents comparable to the HgCdTe benchmark (Rule07) have been observed and the quantum efficiencies of the detectors exceed 30 %. Bias and temperature dependencies of the QE have been studied showing very low turn on bias (~-25mV) and no variation of the peak QE value with temperature. These results show that there are no unintentional barriers in the detector structures and that the diffusion lengths are long enough to provide efficient collection of carriers. Initial results from the extension of the cut-off wavelength from 11 µm to 14 µm are also presented as well as initial results from photodiodes with thicker absorbers to enhance the QE.

Keywords: heterostructure, infrared, detector, superlattice, InAs/GaSb, VLWIR

1. INTRODUCTION

Large size 2D arrays for detection up to about 16 µm are mandatory for future space applications, particularly for weather forecast, climatology and atmospheric sounding missions. The long wave infrared (LWIR, 7-10.5 µm) and very long wave infrared (VLWIR, 10.5-16.0 µm) spectral ranges are crucial for space applications as most of the Earth observation, solar system exploration and astronomical missions require data acquisition in these wavelength ranges. This is particularly true for Earth observation missions, which benefit from simultaneous presence of prominent absorption bands and unique transmission windows in the 7 to 16 µm spectral range. For these missions both high QE and low dark current are required. Mercury-Cadmium-Telluride (MCT) is currently the detector of choice for these applications, however the operability of MCT arrays in this wavelength region is low and the performance of operable pixels degrade with time. The type-II superlattice (T2SL) technology is recognized as the most promising alternative to MCT for 2D LWIR and VLWIR array production. LWIR-VLWIR focal plane arrays (FPAs) using T2SL present many promising benefits such as high uniformity, easier manufacturability [1], greater stability over time [2] whilst also providing high quantum efficiency (QE) and low dark current levels [3]. InAs/GaSb T2SL is the most commonly used T2SL for midwave infrared (MWIR, 3-5µm) and LWIR applications and is currently commercially available as detector arrays up to 640 × 512 pixels, 15 µm pitch and in infrared cameras (for instance by IRNOVA, AIM / Fraunhofer, IAF, SCD, QmagiQ and FLIR).

In this paper, results are presented from the development of FPAs based on InAs/GaSb T2SL for LWIR and VLWIR applications with target cut-off wavelengths of 11.5 µm, 14.5 µm and 16.5 µm and quantum efficiencies exceeding 60%. The intended applications are both for space as well as for commercial applications such as gas detection.

2. EXPERIMENTAL DETAILS

2.1 Material

Structures with three different cut-off wavelengths are presented in this paper. The first structure used for photodiode and detector array development has a cut-off wavelength of 11 µm at 80 K and an absorber thickness of 3.2 µm. The second structure with longer cut-off wavelength (14 µm) also has an absorber thickness of 3.2 µm, while the third structure used for enhanced QE has a 12 µm cut-off wavelength and absorber thickness of 5.1 µm. The photodiode designs have been modelled using a complete set of simulation tools developed by IRnova [4]. Good correlation has been observed between simulations and measured cut-off wavelengths of MBE material grown according to the specified designs, typically the simulated bandgaps of the superlattices are within ± 5 meV of the measured bandgaps of the MBE grown material. The designs of the VLWIR structures used in this study are schematically illustrated in **Figure 1**. These designs are similar to the MWIR epitaxial design reported in [5] and [6], but with the InAs, GaSb and AlSb layer thicknesses of the SLs slightly modified to change the bandgaps to the desired wavelength regions.

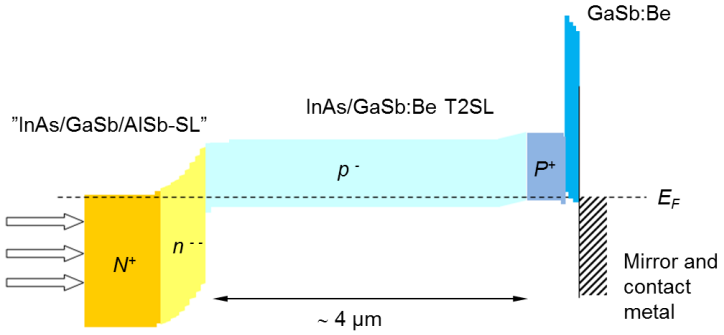

Figure 1. Double heterostructure (DH) detector design used in IRnova's detectors

The measured absorption coefficient of the detector material with 11µm cut-off wavelength is ~1000 cm^{-1} at 10 µm (see **Figure 2a**), which corresponds to 47 % absorption QE in double pass configuration. The PL spectrum shows a strong peak at 11µm, which indicates that the material quality is good (**Figure 2b**).

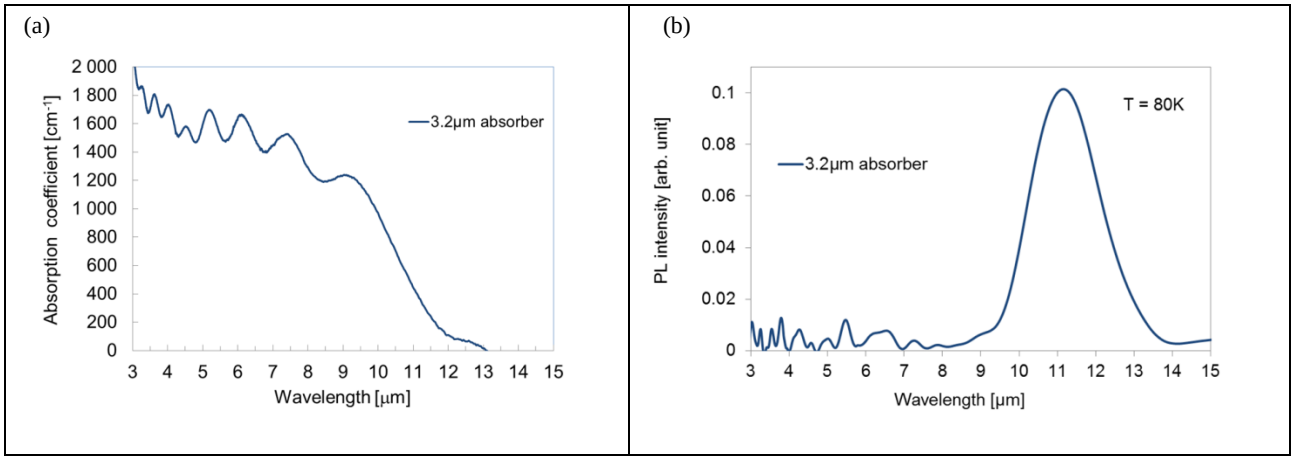

Figure 2. (a) Absorption coefficient and (b) PL spectrum of InAs/GaSb T2SL detector material with 11 µm cut-off wavelength and 3.2 µm thick absorber.

2.2 Fabrication

LWIR and VLWIR single pixel photodiodes and detector arrays were fabricated using standard III/V processing techniques. For single pixel photodiodes, contact photolithography was used to define the pixels, while stepper lithography was used to define the pixels in the detector array fabrication. For both single pixels and detector arrays, pixels were formed by a combination of dry and wet etching [7] and passivated using a dielectric passivation [8]. Top and bottom contact metal and indium bumps (only for detector arrays) were evaporated onto the pixels before dicing. The arrays were then hybridized to fan-out chips (Silicon chip with surface metallic pattern identical to a read out integrated circuit (ROIC)), underfill was deposited and finally the GaSb substrate was fully removed.

3. RESULTS

3.1 Photodiode - quantum efficiency

The temperature dependence of the QE was studied for the 11µm photodiodes, both with respect to spectral response and versus applied bias (**Figure 3a** and **3b,** respectively). From spectral response measurements, a QE of ~30% (at 10 µm) is observed (without AR coating) and it shows just a minor variation of the QE peak values with temperature. This weak temperature dependence indicates that the diffusion length is long enough to collect all carriers generated in the structure. With AR coating, the QE will increase up to ~ 45 %, which is in good agreement with the measured absorption QE for double pass configuration. This further corroborates that there is an efficient carrier collection in the structure.

The turn on bias of the device with 3.2 µm absorber thickness was studied in the temperature range 40 K – 80 K. Very low turn-on bias was observed, on the order of -25 mV at all temperatures (**Figure 3b**). This indicates that there is **no** unintentional barrier in the conduction band that prevents minority carriers from passing the pn-junction.

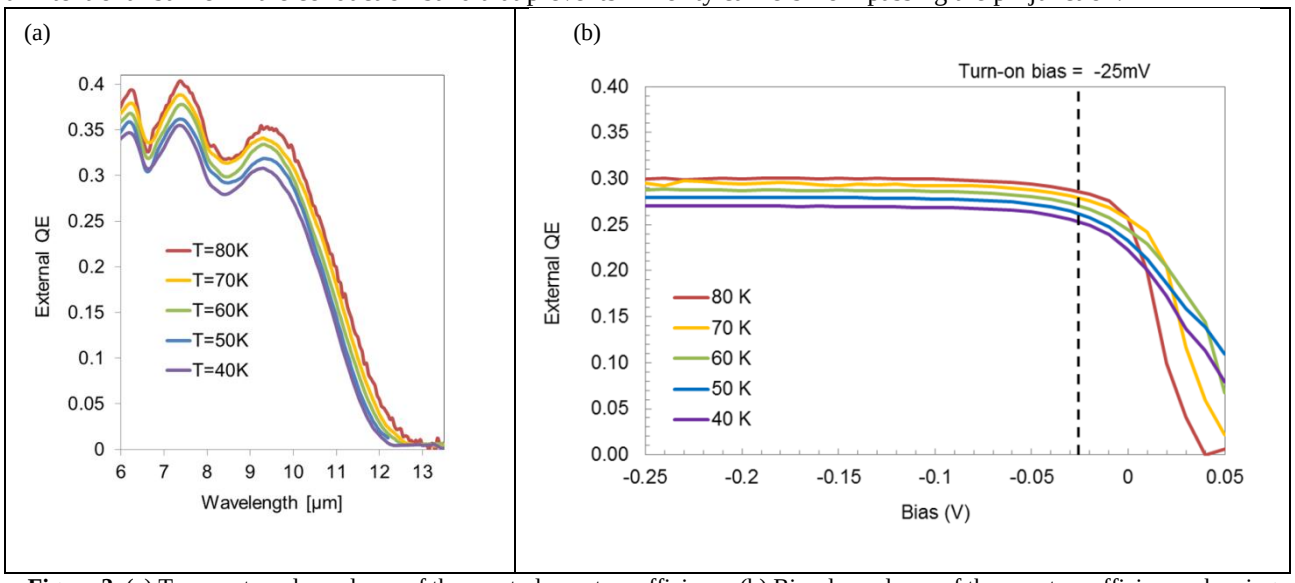

Figure 3. (a) Temperature dependence of the spectral quantum efficiency (b) Bias dependence of the quantum efficiency showing turn-on bias of ~ -25 mV. The cut-off wavelength of the photodiode is 11 µm and the absorber thickness 3.2 µm.

3.2 Photodiode - dark current density

The dark current density was studied for temperatures between 40 K and 80 K, for 30 µm and 60 µm devices. A continuous decrease of the dark current density was observed and the dark current density is bulk limited in the whole temperature range for biases down to -0.3 V (**Figure 4a**). Furthermore, excellent uniformity of the dark current density was observed (**Figure 4b**), with almost identical dark current densities for all $(30\ \mu m)^2$ and $(60\ \mu m)^2$ mesas. The high uniformity and the low dark current density give proof to a well working passivation for these devices.

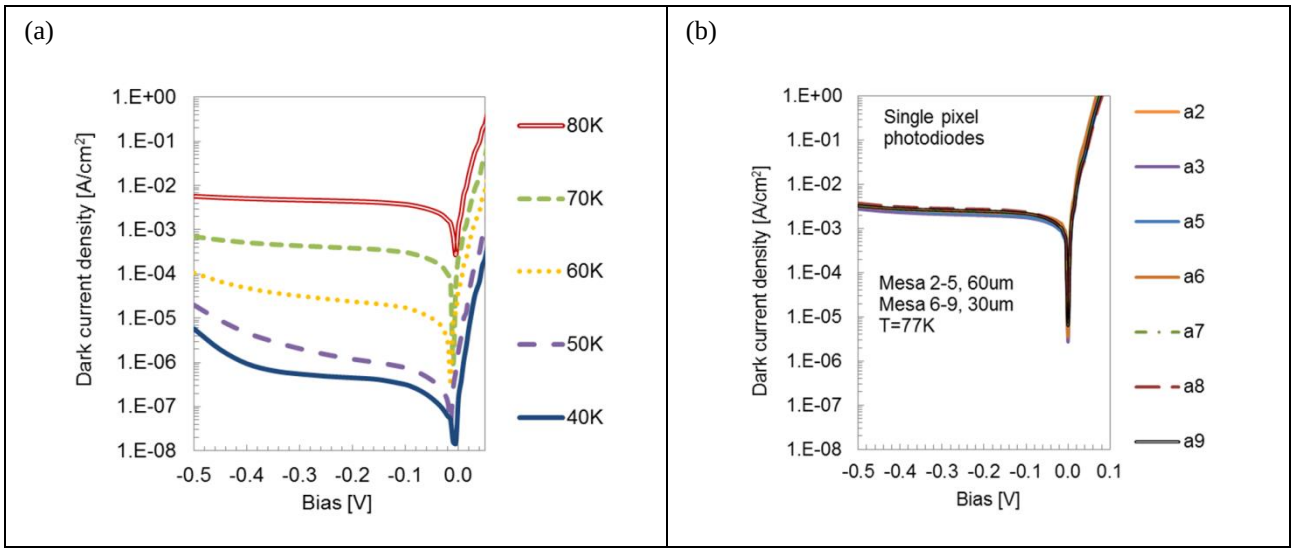

Figure 4. (a) Dark current density vs applied bias in the temperature range 40 K – 80 K for a 30 µm × 30 µm photodiode. (b) Dark current densities of several different 30×30 µm^2 and 60×60 µm^2 photodiodes at 77K, showing good uniformity between diodes.

3.3 Detector arrays - dark current density

30 µm pitch detector arrays, with 26 µm pixels, were fabricated using similar passivation and fabrication techniques as for the single pixel photodiodes. As a first evaluation of the array performance, a detector array was hybridzed to a patterned silicon chip (fanout chip), using the standard hybridization, underfill and substrate thinning techniques normally used in FPA manufacturing at IRnova. The dark current density of pixels in one of these arrays is shown in **Figure 5**. At lower temperatures the pixels in the array are affected by tunneling dark current (**Figure 5a),** which was not the case for the single pixel photodiodes. However, the dark current still exhibits a strong decrease with temperature and the dark current level at the operating bias is comparable to the level of the single pixel devices (**Figure 5b).** This shows that the passivation is still functional after hybridization, underfill and thinning of the substrate. The next step is to hybridize the detector arrays to ROICs for full evaluation of the FPA performance.

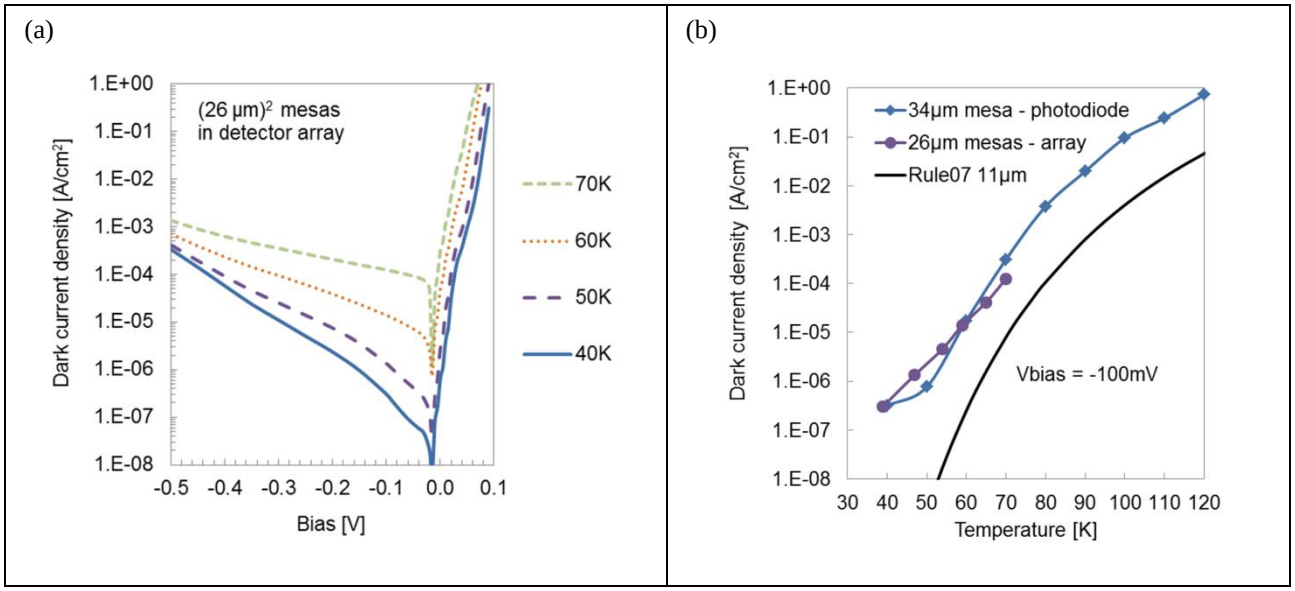

Figure 5. (a) Dark current density vs applied bias in temperature range 40 – 80 K for pixels in a detector array. (b) Dark current density versus temperature for a single pixel photodiode compared to pixels in a detector array after hybridization, underfill and thinning of the substrate.

3.4 Photodiode – longer cut-off wavelength

Very promising results have been obtained from the development of the VLWIR FPAs with longer cut-off wavelengths. Photodiodes with 14 µm cut-off wavelength exhibit almost no temperature dependence of the quantum efficiency in the temperature range 45 K- 60 K (**Figure 6a**). This indicates that the diffusion length is longer than the absorber thickness also for this cut-off wavelength. The turn-on bias is slightly higher in this structure (-0.3 V, see **Figure 6b**), due to an unintentional barrier caused by a too high doping level in the barrier. This can easily be adjusted in the following development. The quantum efficiency observed for this structure is ~20% at 10 µm (without AR-coating) so the structure would benefit from an increased absorber thickness, as will be described in section 3.5.

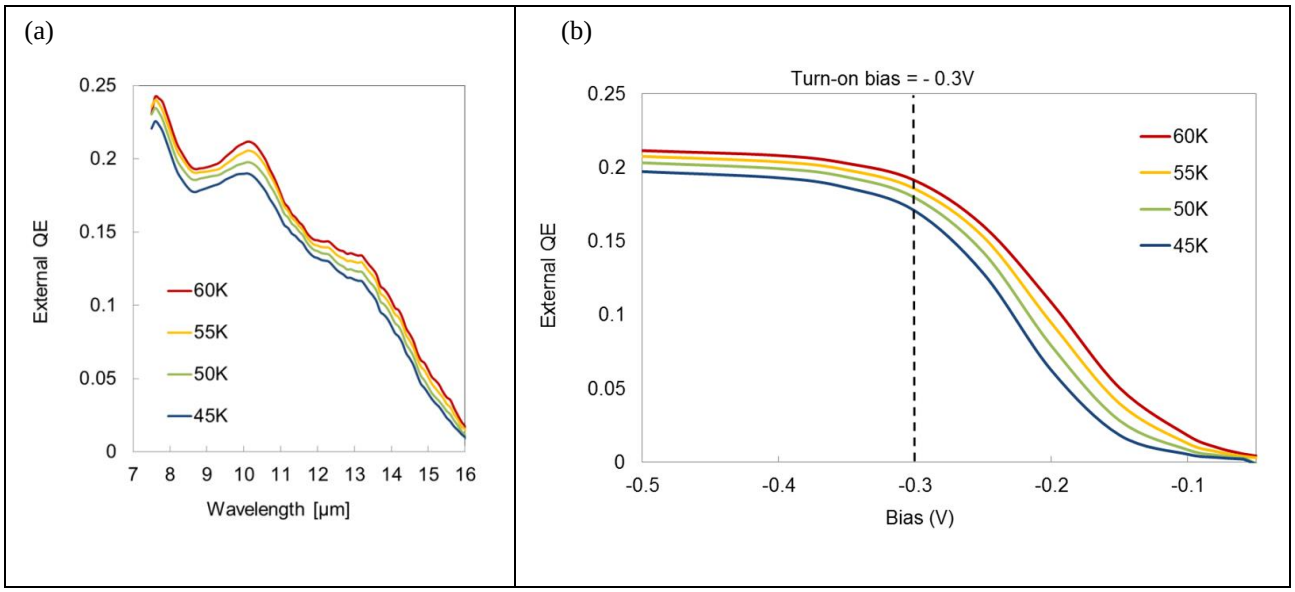

Figure 6. (a) Temperature dependence of the spectral quantum efficiency (b) Bias dependence of the quantum efficiency showing turn-on bias of ~ -300 mV. The 50% cut-off wavelength of the photodiode is 14 µm and the absorber thickness 3.2 µm.

The behavior of the dark current density for the photodiodes with 14 µm cut-off wavelength is similar to the 11 µm ones. As the bias is increased beyond the turn-on bias (-0.3 V) a diffusion limited behavior is observed with continuously decreasing dark current density with decreasing temperature (**Figure 7a**). When studying the temperature dependence of the photodiodes, both 30 µm and 60 µm sized photodiodes follow the Rule07 trend line closely (**Figure 7b**). These results show that there is no problem with surface leakage even for this long cut-off wavelength.

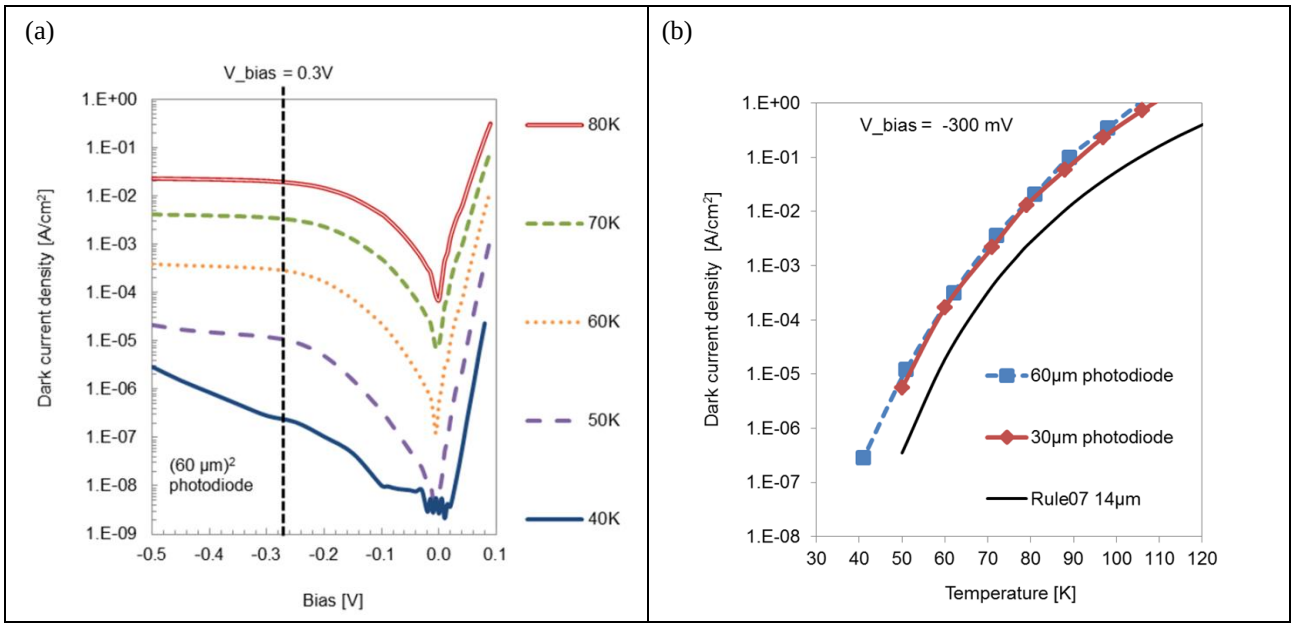

Figure 7. (a) Dark current density versus applied bias and (b) Temperature dependence of the dark current density for a photodiode with 14 µm cut-off wavelength with areas of $(30\ \mu m)^2$ and $(60\ \mu m)^2$ compared to Rule07.

3.5 Photodiode – enhanced QE

In order to further enhance the quantum efficiency of the photodiodes, a detector structure with thicker absorber (5.1 µm) was grown. The measured absorption coefficient and the PL peak position shows a cut-off wavelength of 12 µm, close to the intended cut-off wavelength of 11.5 µm (**Figure 8a**). Enhancement of the QE of up to 45% at 11 µm was observed (without AR coating), enabled by the thicker absorber. By adding an AR-coating, QE values > 60% may be obtained with this structure. The photodiode does however show a strong temperature dependence of the QE (**Figure 8b**). The strong temperature dependence indicates that the diffusion length is shorter than the absorber thickness in this sample. Optimization of the design and growth conditions needs to be performed to increase the diffusion length, in order to benefit from the increased absorption in the detector also at lower temperatures.

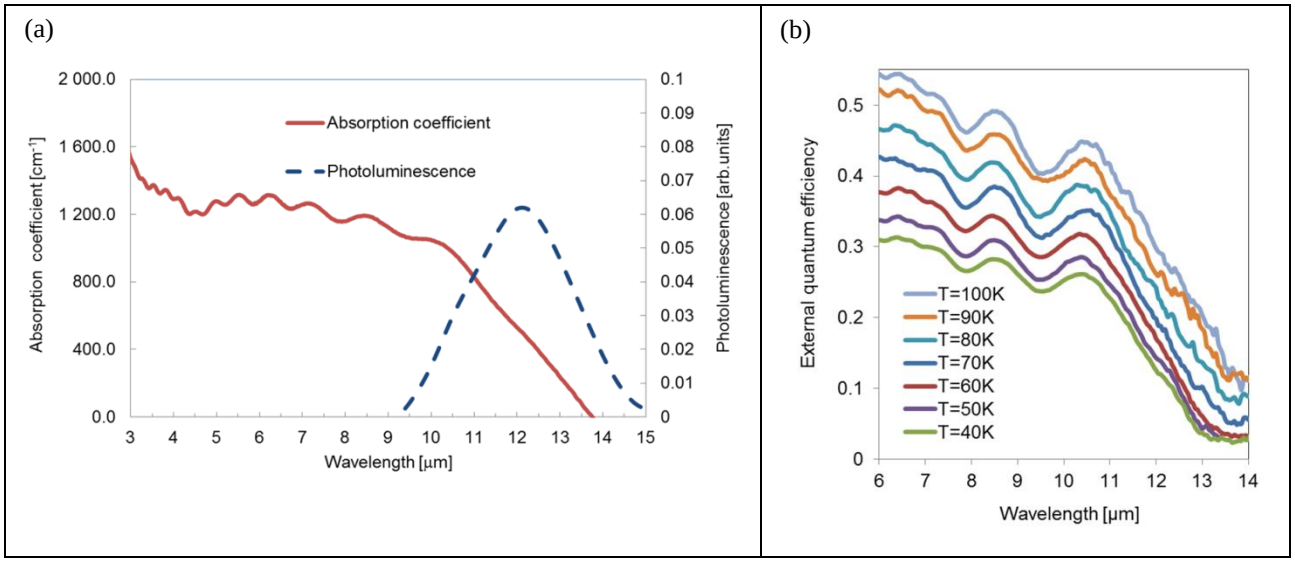

Figure 8. (a) Absorption coefficient and PL spectrum of the 12 µm cut-off wavelength detector material (b). Temperature dependence of the spectral quantum efficiency of a photodiode with 5.1 µm thick absorber

4. SUMMARY

In this article, results from the development of InAs/GaSb photodiodes and detector arrays with cut-off wavelengths of 11 µm, 12 µm and 14 µm have been presented. The dark current levels are comparable to the MCT Rule07 and quantum efficiencies on the order of 30% have been obtained with 3.2 µm thick absorbers and QEs up to 45% have been obtained with thicker detector structures (without AR-coating). With thick absorbers and with AR coating, quantum efficiencies > 60% are anticipated. Furthermore low turn-on bias and almost negligible temperature dependence of the quantum efficiency have been demonstrated. Good uniformity between different pixels has been observed, which is a great advantage for fabrication of large size LWIR-VLWIR FPAs. These performance levels in combination with the radiometric stability over time observed for T2SL FPAs make this technology an attractive alternative to the current state of the art technologies.

5. ACKNOWLEDGEMENTS

We would like to thank ESA for sponsoring this work on VLWIR superlattice detectors in the project 'Low Dark Current VLWIR Type 2 Superlattices (T2SL) InfraRed Detectors', contract number 4000116260/16/NL/BJ.

REFERENCES

[1] Höglund, L., Asplund, C., Marcks von Würtemberg, R., Kataria, H., Gamfeldt, A., Smuk, S., Costard, E. "Manufacturability of type-II InAs/GaSb superlattice detectors for infrared imaging" Infrared Physics & Technology 84, 28-32 (2017)

[2] Nghiem, J., Giard, E., Delmas, M., Rodriguez. J.B., Christol, P., Caes, M., Martijn, H., Costard, E., Ribet-Mohamed, I. "Radiometric Characterization of Type-II InAs/GaSb Superlattice (T2SL) Midwave Infrared Photodetectors and Focal Plane Arrays" Proc. SPIE , International Conference on Space Optics — ICSO 2016, 10562, 105623Y (2017)

[3] Höglund, L., Marcks von Würtemberg, R., Asplund, C., Kataria, H., Gamfeldt, A., Costard, E."T2SL production and development at IRnova – from MWIR to VLWIR detection". Proc. SPIE 10177, Infrared Technology and Applications XLIII, 1017713 (2017)

[4] Asplund, C., Marcks von Würtemberg, R., Höglund, L. "Modeling Tools For Design Of Type-II Superlattice Photodetectors" Infrared Physics & Technology 84, 21-27 (2017)

[5] Asplund, C., Marcks von Würtemberg, R., Lantz, D., Malm, H., Martijn, H., Plis, E., Gautam, N. and Krishna, S. "Performance of mid-wave T2SL detectors with heterojunction barriers" Infrared Physics & Technology 59, 22–27 (2013)

[6] Malm, H., Gamfeldt, A., Marcks von Würtemberg, R., Lantz, D., Asplund, C., Martijn, H. "High image quality type-II Superlattice detector for 3.3 µm detection of volatile organic compounds" Infrared Physics & Technology 70, 34–39 (2015)

[7] Chaghi, R., Cervera, C., Aït-Kaci, H., Grech, P., Rodriguez, J. B. and Christol, P. "Wet etching and chemical polishing of InAs / GaSb superlattice photodiodes" Semicond. Sci. Technol. 24, 065010 (2009)

[8] Martijn, H., Asplund, C., Marcks von Würtemberg, R. and Malm, H.,"High performance MWIR type-II superlattice detectors" Infrared Technology and Applications XXXIX Proc. of SPIE 8704, 87040Z (2013)